PRAMANA
— journal of
physics

Vol. 40, No. 5,
May 1993
pp. 335–343

Simulation of X-ray diffraction patterns for silk fibres using paracrystalline statistics

R SOMASHEKAR and R GOPALKRISHNE URS*
Department of Studies in Physics, University of Mysore, Manasagangotri, Mysore 570006, India
*Department of Applied Physics, National Institute of Engineering, Mysore 570008, India

MS received 23 December 1992

Abstract. Using paracrystalline statistics, we have simulated one-dimensional and three-dimensional X-ray diffraction patterns from natural silk fibres for various values of crystal size and lattice distortion parameters. This is in agreement with the experimental observation of X-ray pattern reported earlier.

Keywords. Silk fibre; paracrystalline statistics; lattice distortion; crystal size.

PACS Nos 61·10; 61·40; 61·00

1. Introduction

As is well known natural polymers like silk fibres have regions of crystalline (ordered) and amorphous (disordered) materials due to the presence of long and flexible molecular chains which hinder further crystallization. Recently [1] research activity has been concentrated on the structural studies of silk fibres because of their importance in industrial applications. Wide angle X-ray scattering pattern from silk fibres consists of a set of broad diffraction peaks scattered by small crystalline regions and several diffuse haloes produced by amorphous materials in the fibre. The random orientation of crystallites around the silk fibre axis, which is essentially a β-pleated structure is understood to produce a cylindrically symmetric pattern. In addition, the peaks become less pronounced and broadens with increasing order of reflection to such an extent that in most cases there is only one order.

The traditional model of polymer structure consists of two phases of high (crystalline) and low (amorphous) electron density. This two-phase model incorporates a statistical variation in size of crystalline and amorphous regions as well as distortion effects within crystallites. The two regions are considered to contribute separately to the X-ray scattering pattern and are unrealistically discontinuous at their boundaries.

The concept of a paracrystal introduced by Hosemann and Bagchi [2] which contains disorder of the second kind, shows much promise in calculation of computed scatterer. It is hoped therefore, that the X-ray diffraction pattern from such a model will not require a separate contribution from an amorphous phase.

Here we look at the theoretical construction of silk fibre model by computing the X-ray scattering from a 3-dimensional finite paracrystal containing disorder of the second kind [3]. The entire probability distribution function is built up from the statistical separation of nearest neighbours in the lattice. At this point no attempt has been made to include other scattering effects.

2. Theory

The lack of information contained in a fibre diffraction pattern means that morphological determination can be achieved by a trial and error method. This enables us to construct a suitable structural model for the fibre and then to calculate the wide angle X-ray scattering intensity pattern.

In paracrystalline statistics the most desirable approach is to calculate the auto correlation function $Q(\mathbf{r})$ of the material. The functional form of $Q(\mathbf{r})$ comes from the inverse Fourier transform of the intensity profile,

$$Q(\mathbf{r}) = \int I(\mathbf{s}) \exp(-i\mathbf{r}\cdot\mathbf{s}) ds$$

$$= \int e(\mathbf{r}_1) e(\mathbf{r}_1 + \mathbf{r}) d\mathbf{r}_1 \tag{1}$$

where $s(=4\pi\sin(\theta)/\lambda)$ is the reciprocal space position vector and $\mathbf{r}$ is the real space vector. $e(\mathbf{r}_1)$ is the electron density of the material. θ is the scattering angle and λ is the wavelength of X-rays. It is important to note, that the auto correlation function at $\mathbf{r}$ of a statistical structure will be determined by the probability of finding scatterers separated by a distance $|\mathbf{r}|$.

2.1 *Paracrystalline probability statistics*

Consider two lattice points somewhere in the infinite 1-*d* paracrystal. The probability $P_1(x)$ that they are separated by a distance x is governed in silk fibres by a weak van der waals and hydrogen bond interaction [4]. The actual form of this interaction is very complex and it is not completely understood. Generally the range of separation of nearest neighbours can be large compared to that of the covalent bonded atom in the chain. There is also a cut off at small distances due to the steep rise in the energy curves. The lattice constant of the crystal m is the mean separation of the lattice points and paracrystallinity g is defined by

$$g^2 = \frac{1}{\langle x \rangle^2} \int_0^\infty |x - \langle x \rangle|^2 P_1(x) dx. \tag{2}$$

In real materials $P_1(x)$ is asymmetric around the mean value due to the shape of the interaction energy curve. Hosemann and Bagchi [2] have shown however that in most cases the asymmetry is not an important factor and a Gaussian approximation to $P_1(x)$ is sufficient. i.e.,

$$P_1(x) = \frac{1}{\omega(2\pi)^{1/2}} \exp\{-1/2(x-m)^2/\omega^2\} \tag{3}$$

where ω^2 is the standard deviation of $P_1(x)$. Using convolution process, the separation of the next nearest neighbours can be determined by propagation of probability and in general for the nth neighbour separation is

$$P_n(x) = \frac{n \text{ times}}{P_1(x) * P_1(x) * \ldots * P_1(x)} \tag{4}$$

$$= \frac{1}{\omega(2\pi n)^{1/2}} \exp\{-1/2(x-nm)^2/n\omega^2\} \tag{5}$$

with $\langle x \rangle_n = nm$ and $g_n^2 = n(\omega/m)^2 = ng^2$.

The dispersion of $P_n(x)$ increases as n increases and is reflected in g_n, which is an important feature of the paracrystal. Separation of nth neighbour becomes very dispersed with the effect of destroying the large range order of the crystal.

Every point in an infinite lattice has two nth nearest neighbour, namely the right $P_n(x)$ and the left $P_{-n}(-x)$. The paracrystal is assumed to be statistically homogeneous so the $P_{-n}(-x) = P_n(x)$. The entire probability distribution $P(x)$, of finding lattice points separated by x in the material is determined by collecting all terms together and can be reduced to

$$P(x) = \delta(x=0) + \sum_{n=1}^{\infty} \{P_n(x) + P_{-n}(-x)\}. \tag{6}$$

The delta function at the origin represents the probability of finding the lattice point at zero distance from itself.

2.2 *The finite 1-d auto correlation function*

A silk fibre can be thought to have a large number of finite scattering units rather than an infinite lattice. The size of the crystallites can have a range of values in the material as a whole. This distribution will not be considered here, but instead we assume that all crystallites have the same size. As we shall see later, the situation then arises that the possible separations of lattice points allowed by equation (5) enables each crystallite to have a different size. We shall consider the effect of this on the auto correlation function and hence the intensity profile.

Firstly the finite auto correlation function will be derived by considering the electron density of finite scatterers. This can be expressed in the following form:

$$e_{\text{finite}}(x) = e_{\infty}(x_1 + x_2) S(x_1) \tag{7}$$

and is shown in figure 1. $S(x_1)$ is the shape amplitude which can be expressed to a first approximation as rectangular function of size d and unit height by

$$\begin{aligned} S(x_1) &= 1 \quad 0 \leqslant x_1 \leqslant d \\ S(x_1) &= 0 \quad 0 > x_1 > d. \end{aligned} \tag{8}$$

Equation (7) includes a separate variable x_2 which enables the origin of the shape amplitude and infinite lattice electron density to be shifted with respect to one another. This allows different regions of the infinite lattice to be positioned within the shape amplitude. The larger number of scattering units can therefore contain different portions of the infinite lattice and will ensure that all possible scattering portions will be present.

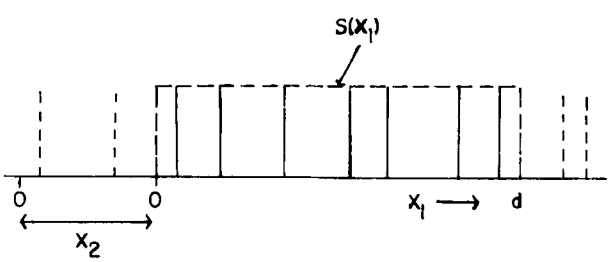

Figure 1. Electron density of a finite paracrystal. All delta functions outside the dotted shape amplitude are neglected. The quantity X_2 allows different portions of the infinite lattice to fall within the shape amplitude.

The auto correlation function in terms of (7) is given by

$$Q_{\text{finite}}(x) = \int_{-\infty}^{\infty}\int_{-\infty}^{\infty} e_{\infty}(x_1 + x_2)e_{\infty}(x + x_1 + x_2)S(x_1)S(x + x_1)\mathrm{d}x_1\mathrm{d}x_2. \tag{9}$$

A contribution to the x_2 integral will occur when there are scatterers positioned at $(x_1 + x_2)$ and $(x + x_1 + x_2)$. Since the probability of finding points separated by x in the lattice as a whole is that of the lattice point probability function $P(x)$, (9) can be simplified using (8) to give

$$Q_{\text{finite}}(x) = Q_{\infty}(x)\int S(x_1)\,S(x + x_1)\mathrm{d}x_1 \tag{10a}$$

with

$$Q_{\text{shape}}(x) = 1 - |x|/\mathrm{d}. \tag{10b}$$

The result in equation (10a) is derived in a similar way to that of Hosemann and Bagchi [2], while Vainshtein [5] use the fact that the auto correlation and intensity are Fourier pair to arrive at the same expression. Substituting equation (10b) and (8) into (10a) the finite 1-D paracrystal auto correlation function is derived to yield

$$\begin{aligned} Q_{\text{finite}}(x) &= 1 - |x|/d\,P(x), \quad |x| < d \\ Q_{\text{finite}}(x) &= 0 \qquad\qquad\quad |x| \geqslant d \end{aligned} \tag{11}$$

2.3 *The intensity profile*

The real part of the complex Fourier transform will yield the scattering profile $I(s)$.

$$I(s) = 2^{*}\,\mathrm{re}\int_{0}^{d}(1 - |x|/d)P(x)\exp(ixs)\mathrm{d}x \tag{12}$$

where $s = 4\pi\sin(\theta)/\lambda$.

It can be shown that the exact solution is

$$I(s) = 1 + \mathrm{re}\sum_{n=1}^{\infty} I_n'(s) \tag{13}$$

where

$$\begin{aligned} I_n'(s) = {} & E(Z_1, Z_2)[(1 - m_n/d) - 2isa_n^2/d]\exp(-a_n^2 s^2 + im_n s) \\ & - 2a_n/d(\pi)^{1/2}[\exp(-m_n^2/4a_n^2) - \exp[-(d - m_n)^2\cos(\mathrm{d}s)/4a_n^2] \end{aligned}$$

and

$$E(Z_1, Z_2) = 2/(\pi)^{1/2}\int_{Z_1}^{Z_2}\exp(-x^2)\mathrm{d}x = \mathrm{erf}(Z_1) - \mathrm{erf}(Z_2),$$

$$Z_1 = -(d - m_n)/2a_n + ia_n s, \quad Z_2 = m_n/2a_n + ia_n s,$$

and

$$a_n^2 = n\omega^2/2, \quad m_n = nm.$$

Unfortunately the above expressions pose several problems to a computational translation because of truncation errors. A reliable method for calculating the complex error function free from truncation errors proved elusive and its properties difficult

to determine. The exact solution of (12) also requires a summation over n as well as series solution to the complex error function.

A correction term for the truncation error has been obtained by making one assumption, i.e., the major contribution to the profile comes from scatterers inside the shape amplitude. The intensity profile produced by N scatterers within the crystallite is then determined by neglecting the contribution from the shape amplitude and the crystallite size is given by $d = Nm$. Mark [6] has obtained an expression for the intensity scattered from a finite 1-D paracrystal as

$$I(s) = 2^* \mathrm{re}[(1 - I^{N+1})/(1 - I) + I\,v/d(1 - I)^2\{I^N(N(1 - I) + 1) - 1\}]^{-1} \tag{14}$$

where $v = 2ia^2 s + m$ and $I = I_1(s)$.

Since the Nth probability peak has its maximum value at d, a modification of the above equation must be made by replacing N with $N - 1$, in (14) and the contribution of $P_N(x)$ is then directly calculated using (13) and is given by

$$I(s) = I_{N-1}(s) + I'_N(s). \tag{15}$$

Here $I'_N(s)$ is the modified intensity for the probability peak centred at d. By substituting $mN = \mathrm{d}$ into equation (13) we arrive at the following result

$$I'_N(s) = (2a_N/d\sqrt{\pi})\exp(ids)[1 - a_N s\{2D(a_N s) + i\sqrt{\pi}\exp(-a_N^2 s^2)\}] \tag{16}$$

with $a_N^2 = N\omega^2/2$.

Here $D(a_N s)$ is Dawson's integral [7] or the error function with a purely complex argument and can be easily computed. We calculate $I_{N-1}(s)$ using the analytic expression (13) and then we add the correction $I'_N(s)$ given above which takes care of the last Gaussian.

2.4 *3-D paracrystal*

For an ideal paracrystal, the lattice vectors form the edges of a parallelopiped and the three dimensional distance probability distribution can be expressed in the following way,

$$P_{hkl}(\mathbf{r}) = \frac{h_{\text{times}}}{P_{100}(\mathbf{r}) * P_{100}(\mathbf{r})} * \frac{k_{\text{times}}}{P_{010}(\mathbf{r}) * P_{010}(\mathbf{r})} * \frac{l_{\text{times}}}{P_{001}(\mathbf{r}) * P_{001}(\mathbf{r})}$$

where $\mathbf{r}$ is the position vector in real space and '$*$' represents a convolution process. Note that the above equation does not include extra terms that allow lattice edges to be non-parallels. In this paper calculations are made for an orthogonal set of axes and we hope in future this can be extended to more general cases.

The 3-D auto correlation function is then obtained from the probability statistics and the intensity by Fourier transformation using an approach similar to the one used in 1-D paracrystal. The expression for intensity can be written using convolution theorem as

$$I(s) = \mathrm{Re}[F\{P_{100}(\mathbf{r})\}]^h [F\{P_{010}(\mathbf{r})\}]^k [F\{P_{001}(\mathbf{r})\}]^l \tag{17}$$

where s is the reciprocal space position vector.

It has been shown already for 1-D that

$$\{F[(1 - x/d_x)\gamma(x)]\}^h = (1 + (i/d_x)\delta/\delta s)^h I_h(s) \tag{18}$$

where $(1 - x/d_x)$ is the shape function and $\gamma(x)$ is the auto correlation function. Extending this to two dimensions we have

$$\{F[(1 - x/d_x)(1 - y/d_y)\gamma(x, y)]\}^{hk} = (1 + (i/d_x)\delta/\delta s)^h (1 + (i/d_y)\delta/\delta t)^k I_{hk}(s, t) \tag{19}$$

and in three dimension we have

$$\{F[(1 - x/d_x)(1 - y/d_y)(1 - z/d_z)\gamma(x, y, z)]\}^{hkl}$$
$$= (1 + (i/d_x)\delta/\delta s)^h (1 + (i/d_y)\delta/\delta t)^k (1 + (i/d_z)\delta/\delta v)^l I_{hkl}(s, t, v). \tag{20}$$

For 3-dimensional statistics, we have

$$I_{hkl}(s, t, v) = \exp\{-q_x^2 s^2\} \exp\{-q_y^2 t^2\} \exp\{-q_z^2 v^2\} \exp(im_x hs)$$
$$\times \exp(im_y kt) \exp(im_z lv) \tag{21}$$

where

$$q_x^2 = a_{11}^2 h + a_{12}^2 k + a_{13}^2 l$$
$$q_y^2 = a_{21}^2 h + a_{22}^2 k + a_{23}^2 l$$
$$q_z^2 = a_{31}^2 h + a_{32}^2 k + a_{33}^2 l$$

and

$$a_{ij}^2 = 1/2\sigma_{ij}^2.$$

Expanding and simplifying we get

$$I(s, t, v) = \sum_l (1 - m_z l/d_z, -2iq_z^2 v/d_z) \exp(-q_z^2 v^2) \exp(im_z lv) \times$$
$$\sum_{hk} (1 - m_x h/d_x, -2iq_x^2 s/d_x)(1 - m_y k/d_y, -2iq_y^2 t/d_y) \times$$
$$\exp(-q_x^2 s^2) \exp(im_x hs) \exp(-q_y^2 t^2) \exp(im_y kt) \tag{22}$$

m_x, m_y, m_z are lattice spacings and d_x, d_y and d_z are crystal sizes in A, a_{ij} are the width of the Gaussian statistics and distortion is given by

$$g_{ij} = sqrt(a_{ij}/m_i).$$

2.5 *Computation*

Silk fibre has orthogonal structure with unit cell parameters $a = 9{\cdot}40$ Å, $b = 6{\cdot}97$ Å and $c = 9{\cdot}20$ Å. Recently we have estimated the number of unit cells and lattice distortions along [210] direction using (210) X-ray reflection from silk fibres employing single order method [8]. Using these parameters, we have simulated X-ray diffraction patterns for one-dimensional lattice using (12) along with the correction equation (16) and it is shown in figure 2 along with an experimental equatorial X-ray diffractometer recording obtained with silk fibres. It is evident from figure 2 that the experimental pattern generated agrees with the observed pattern. To emphasize the fact the crystal size and lattice distortion play an important role in determining broadening of the X-ray diffraction spots, we have simulated X-ray pattern from an 1-D paracrystal for various crystal size and paracrystalline (lattice) distortion values and these are given in figure 2.

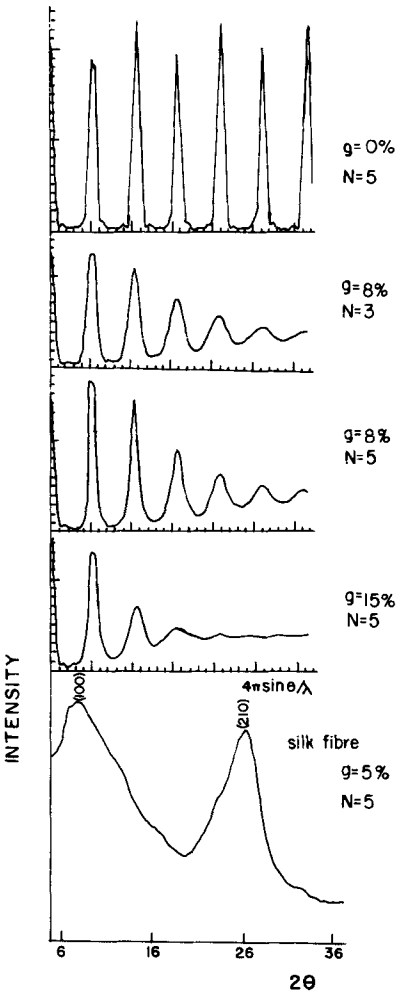

Figure 2. Intensity profiles of a 1-*D* paracrystal having various *g*(lattice distortion) and *N*(crystal units). Generated from the analytical expression including modification as mentioned in the text. XRD recording of a silk fibre is also given.

Our programmes were all written using FTN77 language and executed using Archimedes, 310 M, Acron UK and the computation time was about 1 min.

Extending this to three dimension using (22) we have found that the computation was very time-consuming and hence we have executed the programme using Cyber, University Computer Centre, and the computation time was around 7 to 8 in order to simulate a X-ray Laue type diffraction pattern ($I(s, v)$ vs. s and v). The iso-projection of such a diffraction pattern (only one quadrant) obtained is shown in figure 3. This pattern is nearer to Laue pattern that one normally obtains with silk fibres.

3. Conclusions

We have simulated X-ray diffraction pattern from a silk fibre using probability statistics assuming point scatterers to show the effect of crystal size and lattice distortion in broadening of the X-ray diffraction spots. In fact this can be combined more

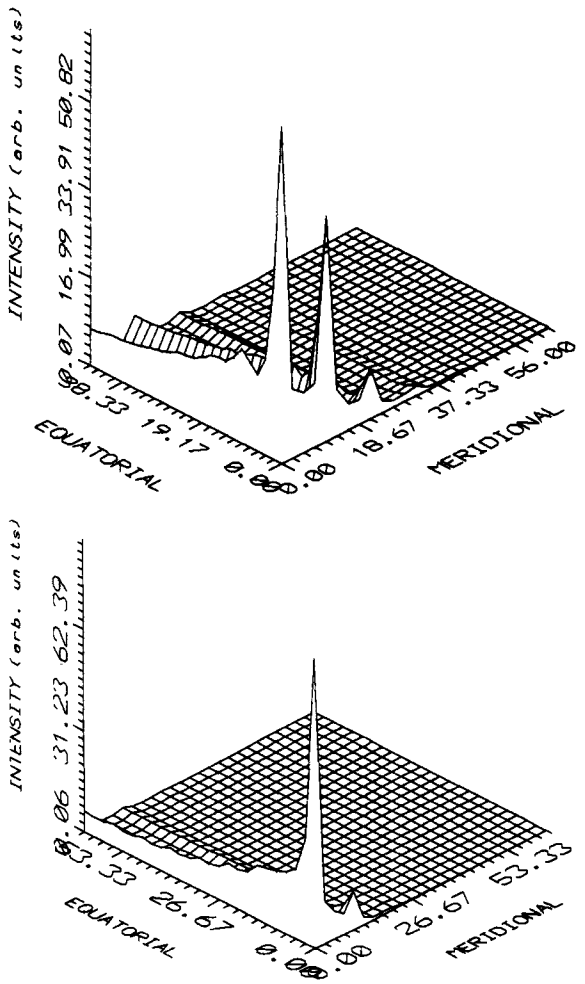

Figure 3. Iso-projection of X-ray diffraction pattern from a 3-D paracrystal for (a) $g = 5\%$ and $N = 5$ units (b) $g = 15\%$ and $N = 5$ units.

rigorously with unit cell structure refinement programme of silk fibre to obtain a more general X-ray diffraction pattern which will be helpful in understanding the silk fibres.

Acknowledgements

The authors thank Dr I H Hall, UMIST, Manchester for initiating the problem and Professor J S Prasad for the necessary help in getting the print out of 3D diagrams. Also authors thank the Systems Manager, University Computer Centre, Mysore for providing the computer facilities.

References

[1] N V Bhat and G S Nadiger, *J. Appl. Polym. Sci.* **25**, 921 (1980)
[2] R Hosemann and S N Bagchi, *Direct analysis of diffraction matter* (North-Holland Publishing company, Amsterdam, 1962)

[3] L E Alexander, *X-ray diffraction methods in polymer science* (Wiley-Interscience, New York, 1969)
[4] J Schutz, *Polymer material science* (Prentice-Hall Inc., New Jersey, USA, 1974)
[5] B K Vainshtein, *Diffraction of X-rays by chain molecules* (Elsevier Publishing Co., London and New York, 1966)
[6] S Mark, *Theoretical model for the wide angle x-ray diffraction pattern of a single crystal using paracrystalline probability statistics* M Sc thesis submitted to University of Manchester, UK (1989)
[7] N N Lebedev, *Special functions and their applications* (Prentice-Hall Inc., New Jersey, USA, 1965)
[8] R Somashekar, R Gopalkrishne Urs and M S Madhava, *J. Appl. Polym. Sci.* **44**, 2161 (1992)